Modeling of Ultrasonic Near-Filed Acoustic Levitation: Resolving Viscous and Acoustic Effects

I. Melikhov[*1], A. Amosov[1], and S. Chivilikhin[2]
[1]Corning Scientific Center, Russia, [2]ITMO University, Russia
*Corresponding author: Corning Scientific Center, 26, lit. A, Shatelena Str., St. Petersburg, 194021, Russia, melikhovif@corning.com

Abstract: Ultrasonic levitation is a developing technology for contactless handling of various objects in certain manufacturing processes where keeping untouched surface is critical. While designing such systems it is important to know an expected lifting force and corresponding levitation height. We focus on the near-filed acoustic levitation when the distance between the floating object and the vibration source is in the order of hundred microns. In this paper we describe a modeling approach which employs simplified equations of air flow in the gap. In contrast to existing models, our model resolves both viscous and acoustic (inertial) effects of the flow. The equation-based mode of COMSOL Multiphysics helps to formulate and solve the governing equations. The model-predicted lifting force is compared to experiment showing good agreement.

Keywords: ultrasonic levitation, core functionality.

1. Introduction

Ultrasonic levitation offers new non-contact technologies for industrial use. These applications are typically based on one of two levitation modes. The first one is usually employed for suspension of small particles placed between an acoustic actuator and reflector. Another levitation type works when a levitating object is larger and it floats over an acoustic actuator. Such systems do not require an additional reflector, and the levitation height is usually in the order of hundred microns. In this paper we focus on the second type of levitation, which is often called ultrasonic near-field levitation.

Ultrasonic near-filed levitation is used for non-contact transportation or suspension systems when manufacturing highly precision products. Examination of the systems of different designs was conducted in papers [1-3]. In addition, researchers offered other applications of ultrasonic levitation, such as motor with levitated rotor [4], ultrasonic clutch [5], and journal bearing systems [6]. In spite of the number of experimental work in this field, there is still a lack of theoretical understanding of the air flow in the gap between the levitating object and the actuator.

A straightforward transient numerical calculation is possible [7], but requires large amount of computation resources. Thus simplified approaches are highly appreciated.

The existing analytical models are based on certain simplifications: an acoustic approximation, and a purely viscous model. The first one neglects viscous forces and is applicable for relatively large levitation heights of levitation (more than 50μm), while the second ignores inertial effects and is applicable for small heights (20μm and less). This paper describes a model which covers both viscous and acoustic limits as well as the intermediate viscous-acoustic regime. The model is derived from the general Navier-Stokes with the help of perturbation theory. The final equations are much easier than the original ones, but still require numerical treatment. Here COMSOL Multiphysics shows its power of working with equation-based models. Weak-form expressions and advanced core functionality, such as component coupling, allows elegant solution of the problem.

2. Model

2.1 Problem Description

We consider the air flow in a narrow gap between a planar ultrasonic transducer and a levitating disk (Figure 1). The transducer has vibration amplitude a and circular frequency ω. Its displacement can be written as

$$H_s(t) = a\cos(\omega t). \quad (1)$$

We assume that the levitation disk is motionless. The levitation distance is denoted by H_0. Then the total thickness of the gap is calculated by

$$h(t) = H_0 - H_s(t). \quad (2)$$

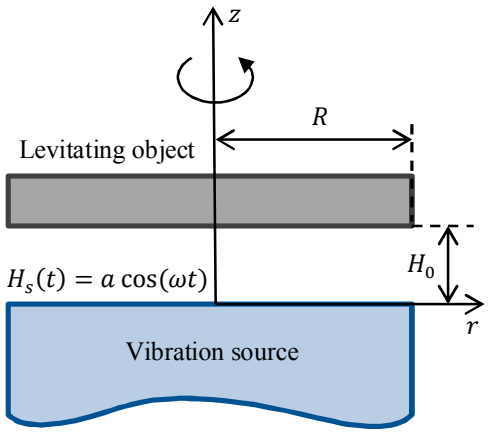

Figure 1. Ultrasonic leviation of a disk.

The air flow in the gap is described by the set of Navier-Stokes equations for compressible gas, the energy equation and the equation of state. In addition, they may be accompanied by viscosity-temperature dependence. The most used one is given by Sutherland's law:

$$\mu = \mu_0 \left(\frac{T}{T_0}\right)^{\frac{3}{2}} \frac{T_0 + C}{T + C}, \quad (3)$$

where μ_0, T_0, and C are empirical constants.

These equations constitute a transient non-linear problem in a narrow region. Such problem requires a lot of computation power. However, the equations can be simplified significantly with the help of perturbation theory.

2.2 Model Overview

The simplified theory is based on the following assumptions:

- the gap thickness is much smaller than the disk radius;
- the gap thickness is much smaller than the acoustic wavelength;
- the vibration amplitude is much smaller than the gap thickness.

The first two assumptions are held for most applications. The last one is used to introduce a perturbation parameter into the model.

These assumptions reduce the energy equation to the adiabatic relation between pressure and density. Together with the ideal gas law and Sutherland's law for the viscosity-temperature dependence it allows expressing density and viscosity in terms of pressure. Further, the assumptions imply zero pressure gradient in z-direction. It allows averaging the continuity equation across the gap reducing the problem dimension.

Next, the solution is sought as a series in the small parameter, the ratio between vibration amplitude and gap thickness. The perturbation technique helps to transform a non-linear problem into a series of linear problems.

The only driving force in the system is the transducer's vibration which is harmonic in time. Thus it is natural to look for the solution in the form of Fourier series in time. The difficulty is that the first-order pressure is harmonic in time, thus it creates zero time-averaged levitating force. Therefore, the equations have to be written out up to the second order. Then the zero-harmonic (i.e. time-averaged) pressure distribution can be calculated.

Finally, the equations should be equipped with proper boundary conditions. There is no reason to solve the air flow outside the gap. In order to imitate the air outflow from the gap we need to set so called non-reflective boundary conditions which allow acoustic wave propagation out of the gap.

2.3 Governing Equations

The steps described in the previous section results in the set of simplified equations. First, we introduce non-dimensional variables as follows:

$$r = \hat{r}/R, \quad z = \hat{z}/H_0, \quad t = \omega\hat{t},$$
$$v_z = \hat{v}_z/(\omega H_0), \quad v_r = \hat{v}_r/(\omega R), \quad p = \hat{p}/p_0,$$
$$\rho = \hat{\rho}/\rho_0, \quad \mu = \hat{\mu}/\mu_0, \quad T = \hat{T}/T_0,$$

where quantities with hat are dimensional, p_0, ρ_0, μ_0, T_0 are pressure, density, viscosity and temperature of air at normal conditions.

In the non-dimensional form the first-order continuity equation in frequency domain is

$$i\frac{p_1}{\gamma} + \frac{1}{r}\frac{\partial}{\partial r}(r\bar{u}_1) = \frac{i}{2}, \quad (4)$$

$$\bar{u}_1 = \int_0^1 u_1\, dz, \quad (5)$$

$$\partial_r p_1|_{r=1} = iKp_1, \quad (6)$$

and the momentum equation is

$$i\gamma K^2 u_1 = -\frac{\partial p_1}{\partial r} + \Sigma\frac{\partial^2 u_1}{\partial z^2}, \quad (7)$$

$$u_1|_{z=0} = u_1|_{z=1} = 0. \quad (8)$$

Here p_1 and u_1 are first-order pressure and radial velocity in frequency domain, i is the

imaginary unit, and γ is the adiabatic index. The non-dimensional coefficients $K^2 = \omega^2 R^2 \rho_0/(\gamma p_0)$ and $\Sigma = \mu_0 \omega R^2/(p_0 H_0^2)$ represent the impact of inertial and viscous effects respectively.

The lateral velocity can be then calculated by integration of the continuity equation:

$$v_1 = -\int_0^z \left(\frac{i}{\gamma} p_1 + \frac{1}{r}\frac{\partial}{\partial r}(r u_1)\right) dz' + \frac{i}{2}. \quad (9)$$

For the second-order quantities the continuity equation for zero frequency takes form:

$$\frac{1}{r}\frac{\partial}{\partial r}\left(r\left\{\bar{u}_2 + \left[\left(\frac{p_1}{\gamma} - 1/2\right)\bar{u}_1\right]_0\right\}\right) = 0, \quad (10)$$

$$\bar{u}_2 = \int_0^1 u_2 dz - (\bar{u}_1 + \bar{u}_1^*)/2, \quad (11)$$

$$p_2|_{r=1} = 0, \quad (12)$$

and the momentum equation is

$$\gamma K^2\left(\frac{i}{\gamma}(p_1 u_{-1}^* - p_{-1}^* u_1) + \left[u_1\frac{\partial u_1}{\partial r} + v_1\frac{\partial u_1}{\partial z}\right]_0\right) = -\frac{\partial p_2}{\partial r} + \Sigma\frac{\partial^2}{\partial z^2}(u_2 + M[p_1 u_1]_0) \quad (13)$$

$$u_2|_{z=0} = -\frac{1}{2}\frac{\partial}{\partial z}[u_1 + u_1^*]_0, \qquad u_2|_{z=1} = 0. \quad (14)$$

Here the constant M comes from Sutherland's law (3):

$$M = \frac{(\gamma - 1)(T_0 + 3C)}{2\gamma(T_0 + C)}. \quad (15)$$

The notation $[\cdot]_0$ denotes zero-harmonic value:

$$[a_1 b_1]_0 = a_1 b_1^* + a_1^* b_1, \quad (16)$$

where a_1, b_1 are first-order quantities, and asterisk corresponds to complex conjugation.

Finally, the total time-averaged levitation force can be calculated by pressure integration over the object's surface:

$$F = \iint p_2 dS. \quad (16)$$

3. Use of COMSOL Multiphysics® Software

The described equations have the advantages that they are linear, have no time dependence, and continuity equation is of lower dimension. On the other hand some difficulties appear such as a need for treatment of imaginary numbers. In addition, projection and extrusion coupling are required to connect variables of different dimensions.

Our COMSOL model includes two consequent stationary study steps. The first one solves first-order equations, and then the second study uses this solution and calculates second-order quantities.

For the examined axisymmetric case the computational domain is a rectangle. The continuity equations (4) and (10) are formulated as *Weak Form Boundary PDE*. These equations are multiplied by the test function corresponding to the pressure. The velocity equations (7), (9), and (13) are solved in the whole domain. The pressure value is extruded from the boundary by *Linear Extrusion* operator. The averaged velocities (5), (11) are calculated by *Linear Projection* operator. The first-order equations (4), (7), (9) with boundary conditions (6), (8) should be solved simultaneously in the same manner as standard Navier-Stokes equations. The same holds for the second-order problem (10), (13) with boundary conditions (12), (14). Note that the boundary condition (14) includes z-derivative of the first-order velocity. In order to resolve it accurately the first-order Dirichlet boundary condition (8) on the bottom boundary are implemented via Lagrange multipliers.

Overall, the model is similar to the built-in implementation of Navier-Stokes equations for laminar flow. The difference is that the pressure may be defined only on the boundary, since its gradient through the gap is negligibly small. Component coupling allows linking the quantities of different dimensions into one model.

It is worth noting that the continuity equations (4) and (10) include only the derivatives along the boundary, while the velocity equations (7) and (13) actually involve only *z*-derivation of the unknown variable. This observation implies that the mesh size in vertical and radial direction may be uncoupled. In our numerical experiments, fifteen elements in *z*-direction are enough for resolving velocity profile, and hundred elements in *r*-direction are sufficient for representing the pressure distribution.

4. Experimental Results and Discussions

The model allows computation of the air flow between the vibration source and the levitating object. For the practical use, the most important is the total levitation force which defines bearing capacity of the system.

4.1 Experimental Setup

In order to validate the model we conducted a series of experiments. The setup is schematically shown on the Figure 2.

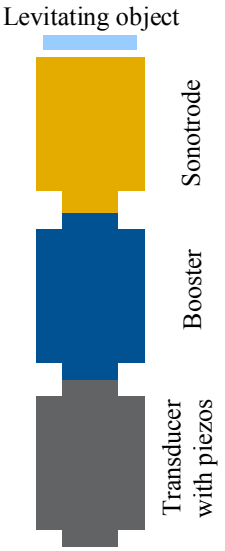

Figure 2. Experimental setup.

Mechanical vibrations are created by the transducer with piezos and then amplified by the booster. The top part, sonotrode, is designed to keep radiating face flat during vibration. The overpressure in the air gap sustains the levitating disk without a contact. The levitation height is measured by an optical sensor.

4.2 Levitation Force

Our model shows that the pressure distribution is highly sensitive to the levitation height, while it only slightly depends on the other parameters, such as vibration frequency, disk radius and others. With the fixed levitation height, a change in the vibration amplitude leads to scaling of the result.

The model was validated against the experiment. The results are summarized on the Figure 3, where the specific weight of a levitating sample, $\sigma = m/(\pi R^2)$, is shown as a function of the levitation distance. It is clear that change in radius does not affect the specific force. On the other hand, varying the vibration amplitude results in shifting (i.e. scaling) the curves.

The root-mean-square error between our model and experiment is 14%.

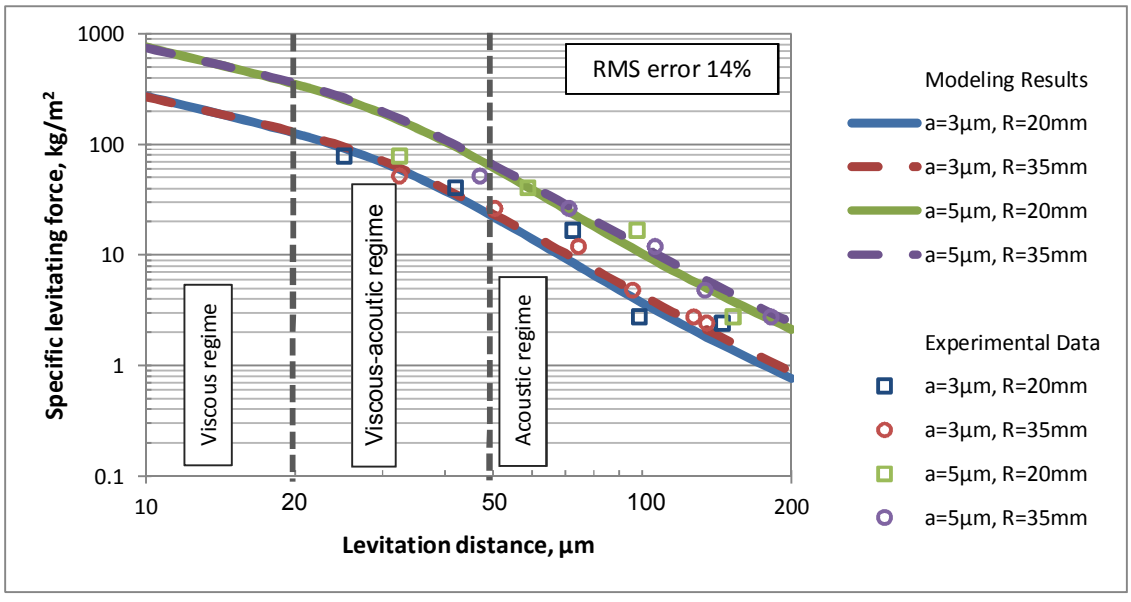

Figure 3. Specific weight of the sample as a function of the levitation distance.

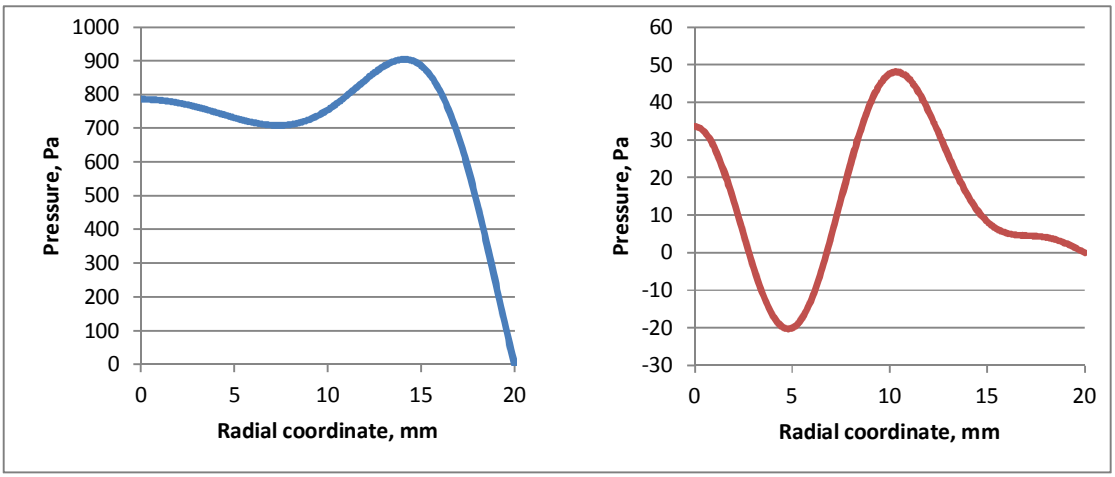

Figure 4. Pressure distribution under a disk of 20mm radius: levitation height 30μm (left) and 150μm (right).

4.3 Pressure Profile

In case of sensitive applications pressure profile may play an important role. Modeling shows that the pressure distribution may vary from close-to-uniform to wavy shape depending on the gap thickness. These two cases are illustrated on the Figure 4.

8. Conclusions

In this paper we demonstrated the model of near-field ultrasonic levitation phenomenon. In contrast to existing simplified models, our model covers a wide range of levitation distances, taking into account inertial as well as viscous effects. COMSOL Multiphysics helps to solve resulting equations in an elegant way.

The model was successfully validated against experiment and therefore can be used for designing ultrasonic suspension systems.

9. References

1. Y. Hashimoto, Y. Koike, and S. Ueha, Near-field acoustic levitation of planar specimens using flexural vibration, *The Journal of Acoustical Society of America*, **100**, 2057-2061 (1996)

2. T. Ide, J. Friend, K. Nakamura, and S. Ueha, A non-contact linear bearing and actuator via ultrasonic levitation, *Sensors and Actuators, A*, **135**, 740-747 (2007)

3. S. Yoshimoto and H. Kobayashi and M. Miyatake, Float characteristics of a squeeze-film air bearing for a linear motion guide using ultrasonic vibration, *Tribology International*, **40**, 503-511 (2007)

4. J. Hu and K. Nakamura and S. Ueha, An analysis of a noncontact ultrasonic motor with an ultrasonically levitated rotor, *Ultrasonics*, **35**, 459-467 (1997)

5. K.-T. Chang, A novel ultrasonic clutch using near-field acoustic levitation, *Ultrasonics*, **43**, 49-55 (2004)

6. S. Zhao and S. Mojrzisch and J. Wallaschek, An ultrasonic levitation journal bearing able to control spindle center position, *Mechanical Systems and Signal Processing*, **36**, 168-181 (2013)

7. H. Nomura, K. Tomoo, and K. Matsuda, Theoretical and experimental examination of near-field acoustic levitation, *The Journal of the Acoustical Society of America*, **111**, 1578-1583 (2002)

10. Acknowledgements

We are thankful to Romain Jeanson, Thierry Dannoux, Ionel Lazer and Pierre Brunello from Corning European Technology Center, Avon, France for their help with experiments.